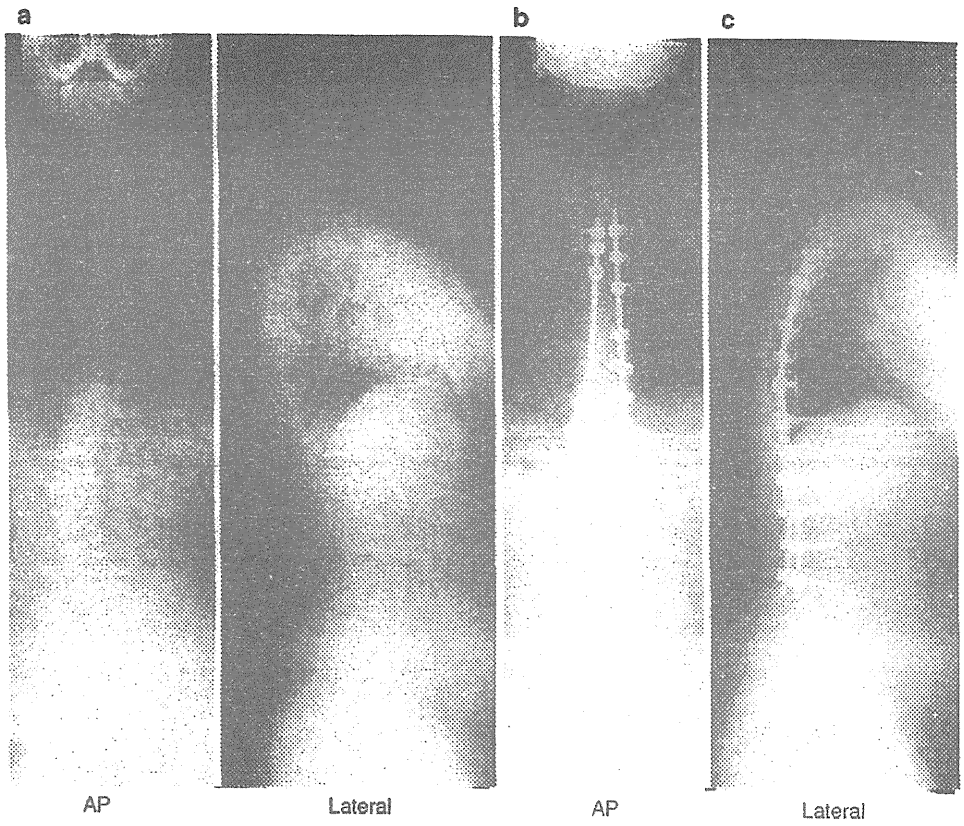

Fig. 2 Case with posterior correction. **a** Before surgery. **b** After surgery. **c** Final follow-up

15q11–13 soon after birth. GH supplement treatment (4 mg/week) and a diet therapy were started when he was 5 years 11 months. Scoliosis was observed in this patient at 7 years of age, and he was subsequently introduced to our Orthopedics Department. The Cobb angle was 37 degrees at T6–L1 at the first consultation. However, the scoliosis deteriorated to a Cobb angle of 55 degrees at T2–L3 and the sagittal alignment was 31 degrees of kyphosis at T1–T12 and 33 degrees of lordosis at L1–S1 at 11 years of age. We tried to use an under-arm brace treatment during the observation period, but he hated the brace owing to his mental retardation and was unable to put it on. At the time of surgery, his height was 148 cm, his weight was 72 kg, his BMI was 15.2 kg/m^2 and he had leptosomatic habitus. There were no abnormal data in blood analyses and no neurological deficits. There were also no abnormal findings by CT or by MRI including anomalies and deformities of the spinal cord and vertebrae. The GH supplement treatment had been performed for 5 years 6 months before surgery. In consideration of his bone fragility, we performed the growing rod method, which can maintain growth, and it was planned with two stages of surgery to produce a stronger anchor. In the first surgery, a hook was anchored in the upper edge region and a screw was attached at the lower edge, and autologous iliac bone was only transplanted on the edges. After 6 months, a strong anchor was confirmed with bone fusion. Next, posterior correction was performed with the Mykres system of spinal instrumentation at T2–L1. A straight tandem connector was used at the thoracolumbar area, and the hook and pedicle screw with the strong anchor through bone fusion were connected with a rod. After this surgery, the scoliosis was corrected to a Cobb angle of 27 degrees and the sagittal alignment was 30 degrees of kyphosis at T1–T12. The quantity of bleeding was 120 ml and the operation time was 2 h 20 min. A doctor from the Department of Pediatrics provided mental support to the patient both preoperatively and postoperatively. Presently, rod extension of 1.5 cm is still being continued every 6 months (Fig. 3).

Discussion

Holm and Laurnen [5] reported that the spinal curvatures in 15–20% of the PWS patients eventually require surgical management. In our study, the frequency of patients who needed surgery was 9.6% (13/136). Accadbled et al. [2] described 16 patients who underwent surgery from 1997 to 2004 for scoliosis in PWS. Regarding complications, there were nine major complications, including four cases of severe kyphosis above the fusion, two deep infections and one transient paraplegia. The four kyphosis cases required

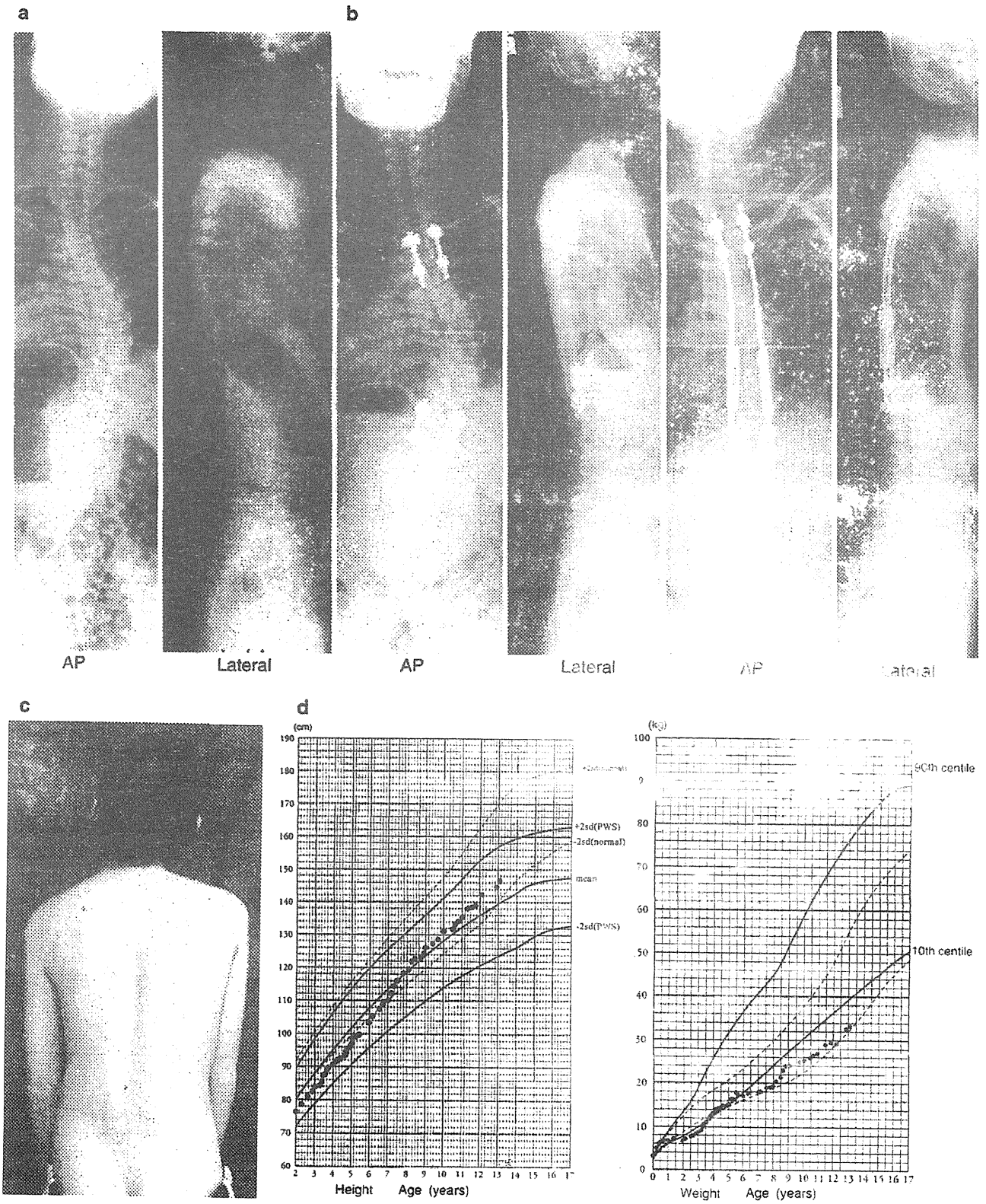

Fig. 3 Case with the growing rod procedure. **a** Preoperative photograph and X-ray. **b** After surgery. **c** Final follow-up. **d** Height in PWS male with respect to age. Weight in PWS male with respect to age

reoperations, three of which were for complications involving permanent spinal cord injury. In that study, GH supplement treatment was administered to 7 of the 16 patients, but most of the patients were obese. Furthermore, the surgeries involved the use of Harrington or Luque instrumentations, which are no longer used.

Weiss and Goodall [6] performed a systematic review in 2009, and concluded that the rate of complications after spinal fusion in patients with scoliosis in PWS was very high and that their death rates were higher than those of patients with adolescent idiopathic scoliosis. Furthermore, the long-term side-effects of the interventions were detrimental, such that the risk–benefit ratios favored conservative approaches over spinal fusion surgery.

As a cause of suffering after surgery for scoliosis in PWS, Rees et al. [1] reported that postoperative respiratory complications can become serious owing to restrictive respiratory disorders caused by the severe obesity peculiar to PWS, deterioration of the quantity of ventilation by the small height and imperfect function of the respiratory muscles with myopathy. Furthermore, they pointed out that preoperative breathing function training is difficult in PWS patients because of their mental retardation. They further stated that a bleeding tendency is brought on by weakness of the blood vessel walls owing to connective tissue abnormalities. In addition, we were concerned about the risk of surgery because there is higher risk of infection associated with the high frequency of diabetes in PWS.

Nohara et al. [7] reported a case of a 14-year-old patient who was severely obese (BMI: 34.4 kg/m^2) and had obstructive pulmonary disease and sleep apnea. After correction surgery, breathing control by a ventilator was required owing to atelectasis for 13 days. In addition, Kakutani et al. [8] described a case of a 17-year-old boy who was severely obese (BMI: 37.5 kg/m^2) and had a Cobb angle of 75 degrees at T10–L3 with a very rigid spinal deformity. In that report, the authors had hoped to operate by anterior release, posterior correction and fusion. However, anterior release was impossible because of a restrictive pulmonary disorder caused by the severe obesity. The authors described that the correction could not be achieved at a satisfactory level, because only posterior correction was able to be performed. However, Tokutomi et al. [9] reported a case of cardiopulmonary impairment caused by severe kyphoscoliosis in PWS. A breathing function imperfection can decrease the quality of life of PWS patients with severe kyphoscoliosis. We need to make a greater effort to improve the surgical outcomes.

On the other hand, Gurd and Thompson [10] described an operation for scoliosis in PWS in a 7-year-old girl. They reported that the girl underwent surgery although her laminas were too weak to hold a Harrington rod. In a recent report from Japan, Yamada et al. [11] reported that a patient with Cobb angles of 43 degrees at T1–T5, 60 degrees at T5–T11 and 52 degrees at T11–L4 was successfully treated surgically using modern instrumentation (XIS-SS system) via a posterior approach. Nohara et al. [7] reported good results in a 12-year-old girl with PWS who had a BMI of 21.4 kg/m^2 and a Cobb angle of the main curve of 106 degrees at T6–L1. A Smith-Petersen osteotomy at T2–L3, anterior release at T7–T12 and correction and fusion at T6–T10 were performed in this patient. After the surgery, the Cobb angle was corrected to 20 degrees and the correction rate was 82%. In addition, Kakutani et al. [8] reported that T12–L3 anterior correction fusion was performed in an 11-year-old girl. Her BMI was 23 kg/m^2 and the quantity of bleeding was 477 ml. Her Cobb angle was corrected to 23 degrees postoperatively from 69 degrees preoperatively without any complications.

There are reports about difficulties associated with management connected with the severe obesity that is peculiar to PWS, as well as difficulties associated with breathing management and mental retardation. Therefore, surgery remains controversial in PWS based on previous reports, considering that there are high rates of complications in patients with PWS undergoing surgery and the health-related benefits of such surgery in these patients are unclear. It is difficult to make clear decisions regarding the optimal approaches for surgical treatment or conservative treatment for PWS patients. Indications for surgery are necessary to determine individual cases.

Recently, the treatment of PWS has improved remarkably in the field of pediatrics. GH supplement treatment was started in Japan in January 2001, and many reports have described its utility and positive effects such as height acceleration, body mass reduction and muscular strength improvement worldwide. However, there are some concerns regarding the risks involved in GH treatment of PWS patients. First, there was a report of sudden death owing to the use of GH treatment [12]. Although the relationship between the sudden death and GH treatment was completely unclear, Nagai et al. [13] subsequently reported that the causes of sudden unexpected death did not differ between PWS patients with or without GH treatment. GH treatment has now become contraindicated for patients who are seriously obese or have a high breathing obstacle. Therefore, careful use of GH treatment is necessary in PWS patients.

Second, the possibility of deterioration in scoliosis was suggested, although we have particularly reported that there was no connection between the frequencies of scoliosis in GH treatment and non-treatment groups [14, 15]. Based on the backgrounds of these studies, GH treatment has recently been recommended at an early age, and it is assumed that its long-term use is not a problem. It is important that PWS patients are treated intensively from 3 years of age, because obesity begins at around this time.

GH supplement treatment is effective for height acquisition, body composition improvement, natural activity and muscular strength improvement, but the greatest purpose of GH use is body composition improvement. All of our patients except one were treated with long-term GH supplement treatment in the Department of Pediatrics from childhood.

Recently, a sex hormone supplement treatment has also been shown to be effective for body composition, mental and bone density improvements. Osteoporosis is caused by imperfect sex hormone secretion in PWS, and this symptom was reported to lead to a risk of more than 29% for a bone fracture once in the lifetime of PWS patients [16]. Preoperatively, improvement in the bone density is important.

Regarding complications, only early dislodgment of the hook and a superior infection were encountered. Fortunately, there were no dangerous complications such as neurological deficits, vascular damage or deep infections. However, an additional operation was performed in two patients. One patient was an 8-year-old girl whose surgery only involved anterior fusion around the apex of the scoliosis to restrain its progression. After 11 years, the kyphoscoliosis had deteriorated at the upper fused level. Accadbled et al. [2] also reported that 4 of 16 patients had progression of serious kyphosis at the upper fused level during their follow-up periods. In our case, the growing rod method was indicated at the present time. In the other case, a screw had been pulled out at the lowest level of the correction level. This patient underwent surgery using sublaminar wiring by a polyethylene tape. However, it was considered that the influence of osteopenia and uncontrolled behavior associated with the mental retardation contributed to the loose screw.

Fortunately, the operative outcomes in our patients were better than in those of some other reports [5, 6]. Some reasons are: first, the Pediatrics Department provided intense preoperative therapy with GH supplement treatment, sex hormone supplement treatment, diet and so on for a long term owing to the completely uncontrolled general conditions in all patients. As a result, the patients had a reduced BMI and improved bone density before surgery. Although breathing function evaluation was difficult because all PWS patients have mental retardation, our patients can be expected to show improvements in their breathing functions. In our patients, we operated using anterior correction fusion. If patients are not obese and do not have breathing function imperfections, surgeons will be able to perform anterior surgery. Therefore, the GH supplement treatment administered was a very effective therapy. In other words, the GH supplement treatment reduced the surgical risk in PWS patients. Consequently, spinal surgeons are able to choose greater ranges of operative methods for successful correction fusion for difficult cases.

Second, in our institution, the spinal surgeons were supported in the preoperative and postoperative therapies by pediatricians who had abundant experience of PWS patients. In addition, there was cooperation by the families of the patients who were well educated about the characteristics of PWS by their pediatricians. Sometimes PWS patients exhibited uncontrolled behavior for orthopedics preoperatively or postoperatively owing to their mental retardation. It is considered that these supports were necessary for smooth treatment. Therefore, the medical team care of orthopedic surgeons and pediatricians was indispensable for the treatment of this disease.

Recently, the dual growing rod technique [17] has been developed. Since all PWS patients have mental retardation, many of them hate brace treatment. In our patients, the brace-wearing rate was low (2/9). When these patients are infants and young children, corrective surgery is required. The dual growing rod technique was found to be an effective method. However, this method requires a lot of distraction surgery to maintain steady growth.

With the development of spinal instrumentation for pediatric surgery, instrumentation for the growing rod method was developed using the strong claw technique, thereby enabling a low profile with an increase in the correction power. In addition, a tandem connector for infants was developed, meaning that the distraction surgery became less invasive. Subsequently, we devised a better technique for the growing rod method of spinal correction, so that we could obtain a strong anchor production for bone fragility in infants or young children. The resulting spinal corrective surgery was separated into two operations. First, anchor production alone was performed with a hook at the upper end, a pedicle screw at the lower end and a bone graft from the autologous iliac bone. After the anchors became strong with complete bone fusion, correction fusion surgery was performed in a second operation.

It is considered that the device for anchor formation that leads to stronger bone fusion was effective for avoiding early dislodgment of the hooks in patients who had bone fragility as infants or young children.

Conclusions

In this study, the frequency of patients with PWS who required surgery in this study was 9.6% (13/136). GH therapy was administered in eight of the nine patients examined who underwent surgery. The mean BMI was 22.5 kg/m^2, and a few obese patients underwent surgery. Regarding complications, one patient experienced early dislodgment of the hook and one patient experienced a superior wound infection. There were no severe complications such as deep infections or neurovascular damage.

Therefore, we consider that GH treatment before surgery may reduce postoperative complications. Brace treatment was only performed in two of the nine patients. The growing rod method was effective for PWS patients who resisted brace treatment owing to mental retardation.

Conflict of interest None of the authors has any potential conflict of interest.

References

1. Rees D, Jones MW, Owen R, Dorgan JC (1989) Scoliosis surgery in the Prader–Willi syndrome. J Bone Jt Surg Br 71(4):685–688
2. Accadbled F, Odent T, Moine A, Chau E, Glorion C, Diene G, de Gauzy JS (2008) Complication of scoliosis surgery in Prader–Willi Syndrome. Spine 33:394–401
3. Obata K, Sakazume S, Yoshino A, Murakami N, Sakuta R (2003) Effects of 5 years growth hormone treatment in patients with Prader–Willi Syndrome. J Pediatr Endocrinol Metab 16:155–162
4. Lenke L, Edwards CC 2nd, Birdwell KH (2003) The Lenke classification of adolescent idiopathic scoliosis: how it organizes curve patterns as a template to perform selective fusions of the spine. Spine 28:199–207
5. Holm VA, Laurnen EL (1981) Prader–Willi syndrome and scoliosis. Develop Med Child Neurol 23:192–201
6. Weiss HR, Goodall D (2009) Scoliosis in patients with Prader Willi syndrome–comparisons of conservative and surgical treatment. Scoliosis 4:10
7. Nohara A, Kawakami N, Miyasaka K et al (2008) Surgical treatment for kyphoscoliosis in Prader–Willi Syndrome (report of two cases). J Jpn Scoliosis Soc 23:41–44 (in Japanese)
8. Kakutani K, Uno K, Kimura T et al (2006) Surgery for scoliosis in Prader–Willi syndrome: report of two cases. J Jpn Scoliosis Soc 21(1):64–67 (in Japanese)
9. Tokutomi T, Chida A, Asano Y, Ishiwata T, Koike Y, Motegi A, Asazuma T, Nonoyama S (2006) A non-obese boy with Prader–Willi Syndrome shows cardiopulmonary impairment due to severe kyphosis. Am J Med Genet Part A 140:1978–1980
10. Gurd AR, Thompson TR (1981) Scoliosis in Prader–Willi syndrome. J Pediatr Orthop 1:317–320
11. Yamada K, Miyamato K, Hosoe H, Mizutani M, Shimizu K (2007) Scoliosis associated with Prader–Willi syndrome. Spine J 7:345–348
12. Eiholzer U, Nordmann Y, l'Allemand D (2004) Fatal outcome of sleep apnoea in PWS during the initial phase of growth hormone treatment. Horm Res Paediatr 58(Suppl 3):24–26
13. Nagai T, Obata K, Tonoki H, Temma S, Murakami N, Katada Y, Yoshino A, Sakazume S, Takahashi E, Sakuta R, Niikawa N (2005) Cause of sudden, unexpected death of Prader–Willi syndrome patients with or without growth hormone treatment. Am J Med Genet Part A 136(1):45–48
14. Nagai T, Obata K, Ogata T, Murakami N, Katada Y, Yoshino A, Sakazume S, Tomita Y, Sakuta R, Niikawa N (2006) Growth hormone therapy and scoliosis in patients with Prader–Willi syndrome. Am J Med Genet Part A 140(15):1623–1627
15. Nakamura Y, Nagai T, Iida T, Ozeki S, Nohara Y (2009) Epidemiological aspects of scoliosis in a cohort of Japanese patients with Prader–Willi syndrome. Spine J 9(10):809–816
16. Butler JV, Whittington JE, Holland AJ, Boer H, Clarke D, Webb T (2002) Prevalence of, and risk factors for, physical ill-health in people with Prader–Willi syndrome: a population-based study. Dev Med Child Neurol 44(4):248–255
17. Akbania BA, Marks DS, Boachie-Adjei O, Thompson AG, Asher MA (2005) Dual growing rod technique for the treatment of progressive early-onset scoliosis. Spine 30:S46–S57

Hum Genet (2012) 131:121–130
DOI 10.1007/s00439-011-1051-4

ORIGINAL INVESTIGATION

Spread of X-chromosome inactivation into chromosome 15 is associated with Prader–Willi syndrome phenotype in a boy with a t(X;15)(p21.1;q11.2) translocation

Satoru Sakazume · Hirofumi Ohashi · Yuki Sasaki · Naoki Harada · Katsumi Nakanishi · Hidenori Sato · Mitsuru Emi · Kazushi Endoh · Ryoichi Sohma · Yasuhiro Kido · Toshiro Nagai · Takeo Kubota

Received: 25 February 2011 / Accepted: 19 June 2011 / Published online: 7 July 2011

Abstract X-chromosome inactivation (XCI) is an essential mechanism in females that compensates for the genome imbalance between females and males. It is known that XCI can spread into an autosome of patients with X;autosome translocations. The subject was a 5-year-old boy with Prader–Willi syndrome (PWS)-like features including hypotonia, hypo-genitalism, hypo-pigmentation, and developmental delay. G-banding, fluorescent in situ hybridization, BrdU-incorporated replication, human androgen receptor gene locus assay, SNP microarrays, ChIP-on-chip assay, bisulfite sequencing, and real-time RT-PCR were performed. Cytogenetic analyses revealed that the karyotype was 46,XY,der(X)t(X;15)(p21.1;q11.2),−15. In the derivative chromosome, the X and half of the chromosome 15 segments showed late replication. The X segment was maternal, and the chromosome 15 region was paternal, indicating its post-zygotic origin. The two chromosome 15s had a biparental origin. The DNA methylation level was relatively high in the region proximal from the breakpoint, and the level decreased toward the middle of the chromosome 15 region; however, scattered areas of hypermethylation were found in the distal region. The promoter regions of the imprinted *SNRPN* and the non-imprinted *OCA2* genes were completely and half methylated, respectively. However, no methylation was found in the adjacent imprinted gene *UBE3A*, which contained a lower density of LINE1 repeats. Our findings suggest that XCI spread into the paternal chromosome 15 led to the aberrant hypermethylation of *SNRPN* and *OCA2* and their decreased expression, which contributes to the PWS-like features and hypo-pigmentation of the patient. To our knowledge, this is the first chromosome-wide methylation study in which the DNA methylation level is demonstrated in an autosome subject to XCI.

Electronic supplementary material The online version of this article (doi:10.1007/s00439-011-1051-4) contains supplementary material, which is available to authorized users.

S. Sakazume (✉) · R. Sohma · Y. Kido · T. Nagai
Division of Pediatrics, Dokkyo University Koshigaya Hospital, 2-1-50 Minami Koshigaya, Koshigaya, Saitama 343-8555, Japan
e-mail: saka343@dokkyomed.ac.jp

H. Ohashi
Division of Genetics, Saitama Children's Medical Center, Hasuda, Japan

Y. Sasaki · N. Harada
Department of Molecular Genetic Research and Analysis, Advanced Medical Science Research Center, Mitsubishi Chemical Medience Corporation, Tokyo, Japan

K. Nakanishi · H. Sato · M. Emi
DNA Chip Research Inc, Yokohama, Japan

H. Sato · M. Emi
Department of Neurology, Hematology, Metabolism, Endocrinology and Diabetology, Yamagata University School of Medicine, Yamagata, Japan

K. Endoh · T. Kubota
Department of Epigenetic Medicine, Faculty of Medicine, Interdisciplinary Graduate School of Medicine and Engineering, University of Yamanashi, Chuo, Japan

Introduction

X-chromosome inactivation (XCI) is a genetic mechanism in females in which one of the two X chromosomes are stochastically inactivated in the early stages of embryonic development. In each cell, the inactivated X-chromosome is randomly chosen; therefore, paternal and maternal X chromosomes have a 50% probability of being inactivated, and females are functional mosaic of two cell populations (Lyon 1961, 1962).

XCI is an essential mechanism for normal development that contributes to gene-dosage compensation process in females (Takagi and Abe 1990). Failure of XCI in females leads to embryonic lethality or abortion on the basis of observations in the embryos of cloned animals (Xue et al. 2002; Yang et al. 2007) or severe phenotypes at birth in humans (Schmidt and Du Sart 1992; Kubota et al. 2002). X-inactivation is mediated by the X inactive-specific transcript gene (*XIST*), a cis-acting RNA molecule (Brown et al. 1991). Studies using ectopic mouse *Xist* integrated into an autosome have demonstrated that *Xist* RNA coats the transgenic autosomes, leading to the reduced expression of genes over 50 cM, and suggest that long-range cis effects occur on the autosome (Herzing et al. 1997; Lee and Jaenisch 1997; Lee et al. 1996). In this report, we describe a boy with t(X;15)(p21.1;q11.2), and analyze the breakpoints, status of the *XIST* gene, extent of XCI spread on an autosome using the DNA methylation status at the CpG islands of genes related to the patient's clinical features. To date, only three studies have measured the spread of X inactivation by gene expression analysis using a somatic cell hybrid that carries the translocated chromosome (Giorda et al. 2008; White et al. 1998) or allele-specific quantitative RT-PCR using heterozygous polymorphism (Sharp et al. 2002). In this report, we investigate how XCI spreads in an autosome using a microarray-based method. To our knowledge, this is the first report that demonstrates the level and extent of XCI in an autosome at a chromosome-wide level in terms of DNA methylation.

Methods

Chromosome and fluorescent in situ hybridization (FISH) analyses

High-resolution G-banded chromosomes were prepared from peripheral blood lymphocytes according to standard procedures. FISH using bacterial artificial chromosome (BAC) DNA as a probe was performed on metaphase chromosomes of the patient with der (X). Chromosome slides were pre-incubated in 2× SSC at 37°C for 30 min, denatured in 70% formamide with 2× SSC at 72°C for 2 min, and then dehydrated at −20°C in ethanol. Cloned DNA was labeled with SpectrumGreen TM-11-dUTP or SpectrumOrange TM-11-dUTP (Vysis, Downers Grove, IL, USA) by nick translation and denatured at 76°C for 10 min. The probe-hybridization mixture (10 mL) was applied to the chromosomes, and they were incubated at 37°C for 16 h. Slides were washed three times in 4× SSC, 0.1% Tween-20 at 45°C and mounted in an anti-fade solution (Vector, Burlingame, CA, USA) containing DAPI.

We used 32 BAC clones to confirm the break point of the X chromosome and to confirm the presence of the *XIST* gene in the der (X). We also used 12 BAC clones to confirm the breakpoint of chromosome 15. The BAC clones, their locations, and the containing gene are shown in Supplemental Table 1. All of the clones were selected using the UCSC genome browser database (http://genome.ucsc.edu).

Quantitative RT-PCR analysis

Total RNA was isolated using the RNeasy Mini Kit (Qiagen, Hilden, Germany) according to the manufacturer's instruction. Reverse transcription and real-time RT-PCR were carried out using SYBR ExScript RT-PCR Kit (Takara, Kyoto, Japan). Quantitative real-time RT-PCR analysis was performed in triplicate with an Applied Biosystems (Foster City, CA, USA) Prism 7700 Sequence detection system according to the manufacturer's instructions. The mRNA expression levels, normalized against those of the corresponding *GAPDH* mRNA levels, were relatively quantified. The primer pairs used for the *GAPDH* and *OCA2* genes were GAPDH (HA031578, Takara) and OCA2 (HA032005, Takara), respectively, and the primer sequences for the *XIST* gene were: XIST-113202F, 5′-GCAGTTTGCCCTACTAGCTCCT-3′ and XIST-11456R, 5′-TCCTCAGGTCTCACATGCTCA-3′.

X-chromosome inactivation analyses

Replication R-banding study was performed on chromosomes stained with DAPI as described elsewhere (Uehara et al. 2001).

The human androgen receptor gene locus (HUMARA) assay using methylation-specific PCR was performed as described previously (Kubota et al. 1999). Briefly, the assay uses a bisulfite-treatment followed by PCR, and we obtained the inactive X pattern based on the methylated allele at the HUMARA locus and the active X pattern based on the unmethylated allele at the same locus. Both patterns were used to calculate the XCI ratio (Kubota et al. 1999).

Methylated DNA immunoprecipitation (MeDIP) assay using a human CpG island microarray

The methylation status of the CpG islands (CGIs) was analyzed using the methylated DNA immunoprecipitation method with a human CGI oligonucleotide microarray system according to the manufacturer's protocol (Agilent Technologies, Santa Clara, CA, USA). Briefly, sonicated genomic DNA was prepared and used for immunoprecipitation with a 5-methylcytidine monoclonal antibody (BI-MECY-1000) (Eurogentec, Seraing, Belgium). We

labeled 250 ng of methylation-enriched DNA samples and reference (input, non-enriched control) DNA samples, which were not amplified, with Cy3 and Cy5, respectively, using an Agilent Genomic DNA Labeling Kit PLUS (Agilent Technologies). Labeled DNA was hybridized to the custom array containing 5,859 high-density probes specific for the CpG promoters on chromosome 15, which was designed using the eArray Agilent web-based database (hg18, NCBI 36.3) on a 44K platform CpG promoter microarray. The array was scanned with an Agilent G2565BA microarray scanner (Agilent Technologies). All experiments were performed in duplicate. We compared methylation between the patient and two normal controls, according to the previously described methodology (Sharp et al. 2010).

Bisulfite DNA sequencing

Genomic DNA was extracted from peripheral lymphocytes, and bisulfite treatment of genomic DNA was performed using the EpiTect Bisulfite Kit (Qiagen) according to the manufacturer's instructions. Primers for the bisulfite genomic sequencing PCR were designed using the online program MethPrimer (http://www.urogene.org/methprimer/index1.html). The amplified PCR products were sequenced using the following primers:

SNRPN-F, 5′-AAAAACTTTAAAACCCAAATTCC-3′;
SNRPN-R, 5′-GTGGGGTTTTAGGGGTTTAGTA-3′;
UBE3A-F, 5′-TTCTAACACCAACCCCTTC-3′;
UBE3A-R, 5′-AGTTTTTY (C and T) GGTGTGGATA GGTA-3′;
OCA2-F, 5′-TGTGTTTGTGTTGTAGGAGGGGT-3′;
OCA2-R, 5′-CCCACAAAACTACCCACATAACC-3′;
UBR1-F, 5′-AATATTTTTTGGGGTTTGTAGGT GA-3′;
UBR1-R, 5′-CAAAACCAACACTAAACAAAACCT C-3′;
TRIP15-F, 5′-GAAAGGGTAAAGTTAGGGTTTAT AT-3′;
and TRIP15-R, 5′-CCTACTTCTCCAACAAAAAAA AA-3′.

Single nucleotide polymorphism (SNP) analysis using a microarray

SNPs on chromosome 15 were analyzed using the Human 317K-Duo Bead chip array, and SNP genotypes were determined using the GenomeStudio software (Illumina, San Diego, CA, USA). More than 317,000 tagSNPs markers on this chip were selected using the database of the International HapMap Project Phase I and Phase II (NCBI build 36.3/hg18).

Genomic search for transposable elements

The UCSC data (NCBI 36.3/hg18) were searched for LINE1 (L1), Mammalian-wide Interspersed Repeat (MIR), and Alu transposable elements using the RepeatMasker Program (Ver. 3.2.7). We focused on the *SNRPN*, *UBE3A*, and *OCA2* genes, and plotted the elements using the R program (Ver. 2.10).

Results

Proband

The male proband was a 5-year-old boy and the only child of healthy and non-consanguineous parents. The pregnancy was not eventful and he was born at the 41st week of gestation and weighed 2,933 g. Body length and head circumference were at the 50th percentile (49 and 35.5 cm, respectively). Hypotonia was prominent and nasogastric tube was required for feeding during the neonatal period. PWS-like dysmorphic features were noted, including small mouth, micrognathia, rocker-bottom feet, hypopigmented hair, cryptorchidism, and hypogenitalism. Abdominal ultrasound revealed a horseshoe kidney, while head MRI demonstrated hypo-plastic corpus callosum and occipital arachnid cyst. He had severe motor developmental delay and spastic quadriplegia: at the age of 20 months he could not control his head and could not roll over. A wheelchair was required to move and continuous drainage of saliva was necessary due to difficulties with swallowing.

Cytogenetic analysis

High-resolution G-banding showed an abnormal karyotype: 46,XY,der(X)t(X;15),−15 in all 50 cells analyzed (Fig. 1a). Karyotypes of both parents were normal (data not shown). To confirm the break point of the derivative X chromosome in the patient, FISH analyses were performed, in which a series of BAC probes to the X chromosome were hybridized on metaphase spreads of the patient's lymphocytes. As a result, the signals from the RP11-172M3 probe (SpectrumOrange), mapping to Xp21.2, and from RP11-134B11 (SpectrumGreen), mapping to Xp21.1, were detected on the normal X chromosome, whereas only signal from RP11-134B11 (SpectrumGreen), mapping to Xp21.1, was detected on the derivative X chromosome, indicating that the break point of the derivative X was located between these probes (Xp21.2-p21.1 region) (Fig. 1b). Likewise, the signals from the RP11-79C23 probe (SpectrumOrange), mapping to 15q11.1-11.2, and from RP11-357P4 (SpectrumGreen), mapping to 15q11.2, were detected on the normal chromosome 15, whereas only signal from RP11-357P41 (SpectrumGreen), mapping to 15q11.2, was detected on the

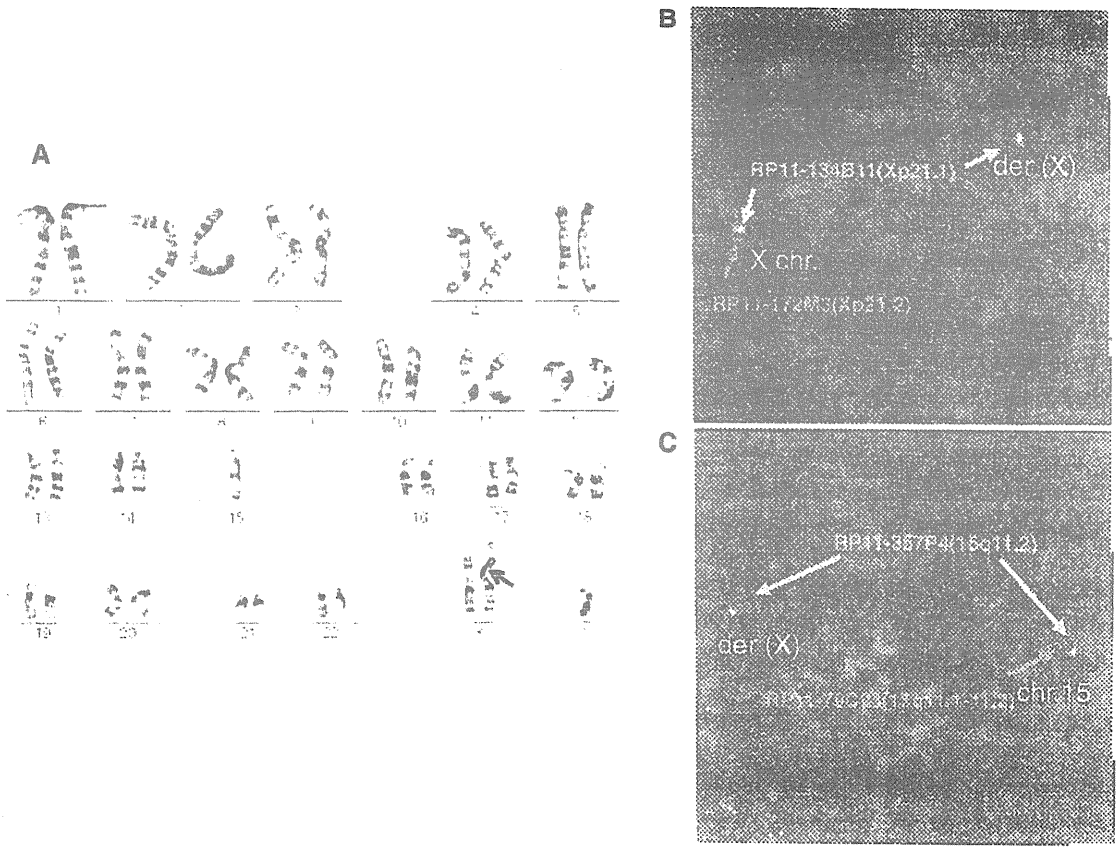

Fig. 1 Cytogenetic analyses of the patient. a GTG-banded full karyotype of the patient. No mosaicism was found in the 50 cells examined. An *arrow* indicates the breakpoint of the derivative X chromosome. b FISH analysis using the RP11-172M3 probe (SpectrumOrange) at Xp21.2 (a signal shown in *red*) and the RP11-134B11 probe (SpectrumGreen) at Xp21.1 (two signals shown in *green*). The presence of a *green* signal, but not a *red* signal, in the derivative X chromosome (der (X)) indicate that the breakpoint is located between the two probes (Xp21.2-p21.1). c FISH analysis using the RP11-79C23 probe (SpectrumOrange) at 15q11.1-q11.2 (a signal shown in *red*) and the RP11-357P4 probe (SpectrumGreen) at 15q11.2 (two signals shown in *green*). The presence of a *green* signal, but not a *red* signal, in the derivative X chromosome (der (X)) indicate that the breakpoint is located between the two probes (15q11.1-q11.2)

derivative X chromosome, indicating that the break point of the derivative X was located between these probes (15q11.2) (Fig. 1c). Taken together, the patient's karyotype was interpreted as 46,XY,der(X)t(X;15)(p21.1;q11.2),−15.

SNP analysis of chromosome 15

To determine the parental origin of the chromosomes 15 in the patient, we examined the 9303 SNPs on chromosome 15 and found that 444 SNPs demonstrated the biparental inheritance of chromosome 15 in the patient (Table S2). The remaining SNPs were uninformative and none showed uniparental origin. Since the SNRPN gene promoter region was extremely methylated, in which the normally unmethylated paternal allele was methylated presumably due to XCI, the chromosome 15 region in the derivative X was determined to be of paternal origin. Therefore, together with the results of the HUMARA assay, in which the normal X and derivative X chromosomes were maternal, SNP analysis suggests that the derivative X consisted of the maternal X chromosome and the paternal chromosome 15.

X-chromosome inactivation analysis

To examine the XCI status in the derivative X chromosome, we first performed FISH analysis with a BAC probe containing the *XIST* gene to confirm its presence. As a result, the signal from the BAC probe RP11-13M9 (SpectrumGreen) was retained in the normal and derivative X chromosomes, as was the signal from the X-chromosome control probe RP11-402H20 (SpectrumOrange) at the Xq subtelomeric region (Fig. 2a). Replication R banding analysis demonstrated that the derivative X chromosome was inactivated, and this inactivation covered the X chromosome and the proximal 15q region; however, the inactivation did not spread distal to 15q in all the 100 cells

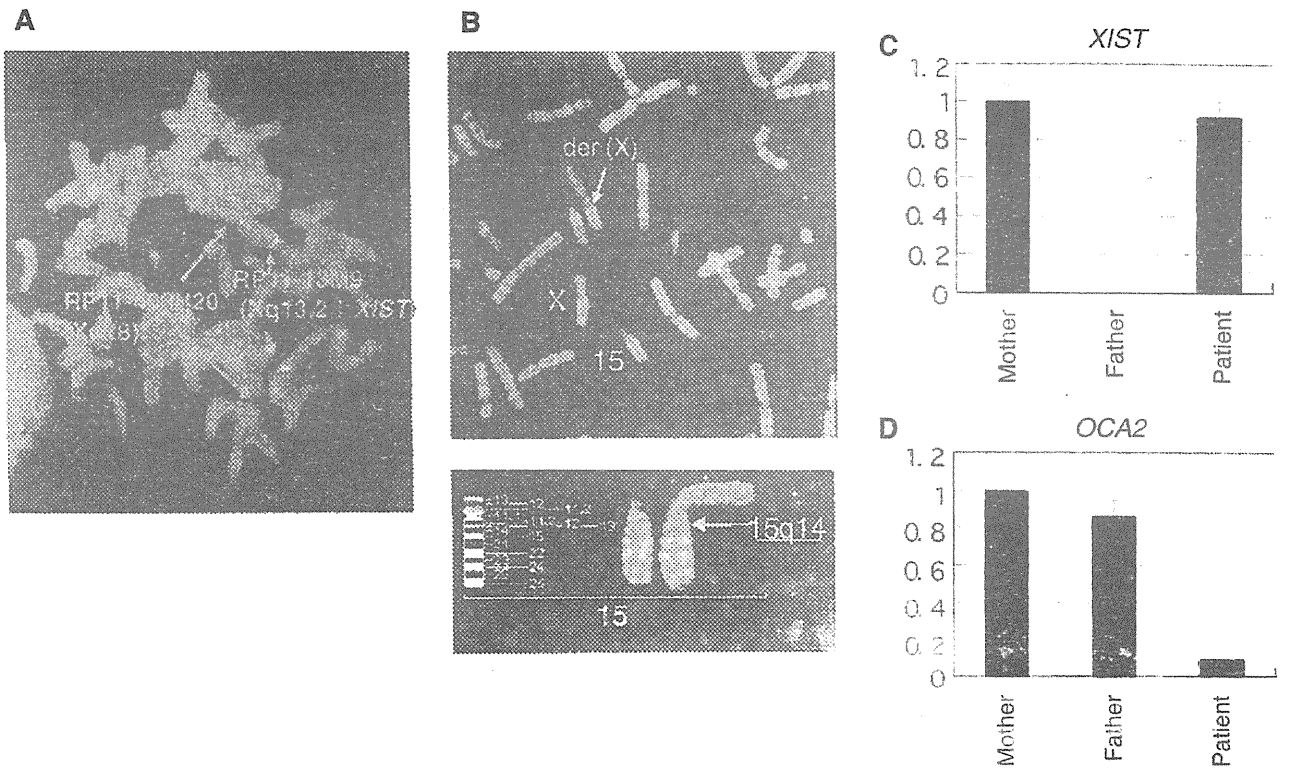

Fig. 2 Cytogenetic analysis for X-chromosome inactivation. **a** FISH analysis using the RP11-13M9 probe (SpectrumGreen), covering the *XIST* gene (two signals shown in *green*) and the RP11-402H20 probe (SpectrumOrange), located at the Xq-subtelomeric region (two signals shown in *red*), indicating that the derivative and normal X chromosomes have an *XIST* gene. **b** Replication R-banding study in the patient. A late replication/no banded segment was observed in the derivative X chromosome beyond the 15q14 region, which was assessed by the R-banding pattern of the normal chromosome 15 (see *lower enlarged panel*). **c** Real-time RT-PCR assay for *XIST* gene expression in the patient and parents. **d** Real-time RT-PCR assay for *OCA2* gene expression in the patient and parents. The *axis* represents the relative expression level for the mother (**c**, **d**)

examined (Fig. 2b, upper and lower panels with enlargement). We also confirmed *XIST* gene expression in the patient using real-time RT-PCR at almost the same level as in the mother, a normal female (Fig. 2c), suggesting *XIST* expression from the allele on the derivative X chromosome.

The HUMARA assay showed that the patient had a relatively non-random (skewed) XCI pattern (89:11) whereas the mother had a random XCI pattern (41:59). In addition, two copies of the HUMARA gene locus (Xq12) were inherited from the mother and no copy was inherited from the father (Fig. 3). These data indicate that the XIST gene was expressed from the derivative X, leading to the XCI effect spreading to the middle of the chromosome 15 in the derivative X beyond the break point, and also indicate that the normal and derivative X chromosomes were transmitted from the mother. The relatively skewed inactivation pattern in the patient was consistent with the result of the replication study, in which one X (presumably the derivative X) was preferentially inactivated in all cells examined.

DNA methylation analyses of CGIs on chromosome 15 of the derivative X chromosome

To further understand the spread of XCI on the chromosome 15 of the derivative X in terms of DNA methylation, we performed MeDIP analysis using CGI microarray to identify CGI hypermethylated regions in the patient in comparison with two healthy male controls (Fig. 4, upper panel). As a result, we observed constant CGI hypermethylation from the break point, beyond the *OCA2* locus (15q12), to 15q14 [40 Mb from the centromere]. In the middle of 15q, from 15q21.1 [50 Mb] to 15q22.2 [60 Mb], including *UBR1* (15q15.2) and *TRIP15* (15q21.1), CGI hypermethylation was rarely detected. However, scattered CGI hypermethylation was observed in the remaining telomeric region distal to 15q22.2 [60 Mb] in the patient (Fig. 4, upper panel).

In the proximal region, the CGIs of *SNRPN*, *ATP10A*, and *OCA2* were hypermethylated in the patient, whereas that of *UBE3A*, which was located in the middle of these

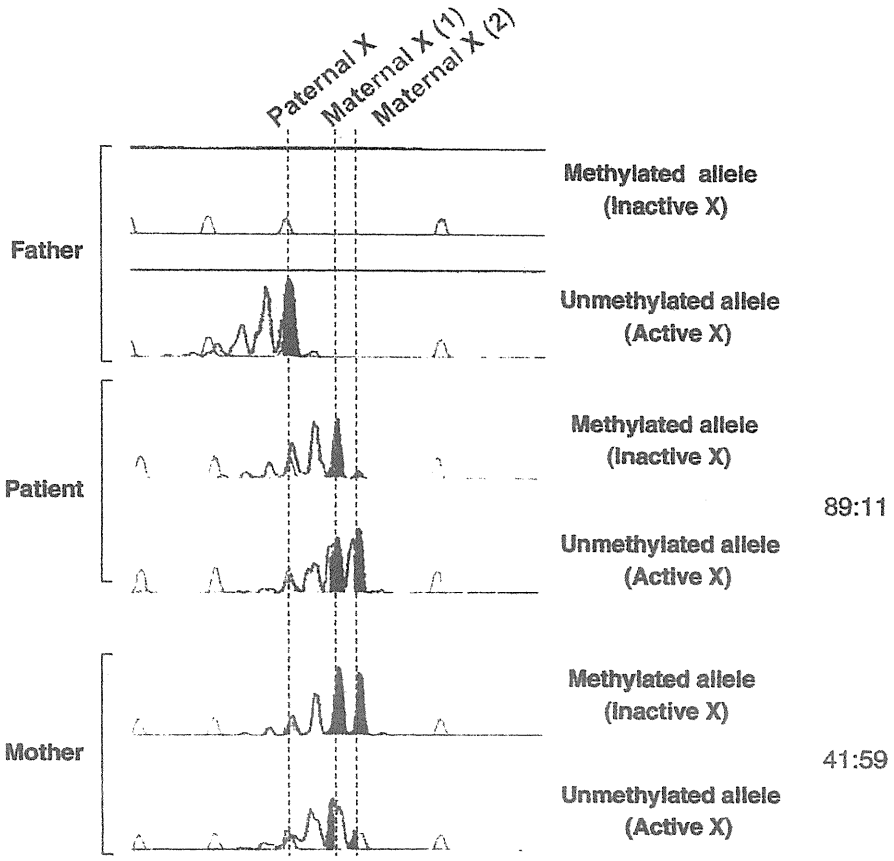

Fig. 3 Molecular analysis of X-chromosome inactivation. The HUMARA assay, based on methylation-specific PCR, demonstrates that the peak area of "Maternal X (1)" is much larger than that of "Maternal X (2)" in the methylated allele (Inactive X) lane in the patient, indicating relatively non-random (skewed) inactivation (89:11). However, the peak area of "Maternal X (1)" is affected by a shadow peak of "Maternal X (2)" in the unmethylated allele (Active X) lane, by PCR slippage error at the triplet repeat locus, because the allele difference between "Maternal X (1)" and "Maternal X (2)" is only 3 base pairs (1 triplet). Therefore, in this case, we only consider the result in the methylated allele (Inactive X) lane. In the mother, the patterns of the peak area of "Maternal X (1)" and "Maternal X (2)" are similar between the methylated (Inactive X) and unmethylated allele (Active X) lanes, indicating random inactivation (41:59). In the father, no peak is detected in the methylated allele (Inactive X) lane and only 1 peak is detected in the unmethylated allele (Active X) lane, as expected

genes, was not hypermethylated (Fig. 4, middle panel). In the middle region, the CGIs of *UBR1* and *TRIP15* were not hypermethylated in the patient (Fig. 4, middle panel).

Bisulfite sequencing analyses confirmed the results obtained from the MeDIP analysis. The CGI of *SNRPN* was extensively hypermethylated in the patient, whereas a healthy control showed ~50% methylation. Since *SNRPN* is an imprinted gene in which only the maternal allele is hypermethylated, this observation suggests that the normally unmethylated paternal allele (presumably the allele on the derivative X) was methylated in the patient (Fig. 3, lower panel). In the CGI of *OCA2*, the patient showed ~50% methylation whereas the control was not methylated, indicating that one of the two alleles (presumably the allele on the derivative X) was hypermethylated in the patient (Fig. 4, lower panel). This observation was consistent with the lower expression level of this gene in the patient (Fig. 2e). Taken together, the CGIs of the genes at 15q11.2-12 were hypermethylated presumably due to the spread of XCI in the derivative X.

However, the CGI of *UBE3A* was not shown to be hypermethylated by either the microarray assay or bisulfite sequencing analysis (Fig. 4, middle and lower panels); however, CGIs of the adjacent genes, *SNRPN* and *ATP10A*, were hypermethylated (Fig. 4, middle panel), indicating that the CGI of *UBE3A* might have some mechanism to escape the X-inactivation effect. We observed a lower density of LINE-1 and Alu elements in the upstream region of UBE3A (GenBank Accession No.: NM_000462) (Fig. 4, light blue area) compared with that in the upstream region of SNRPN (GenBank Accession No.: NM_003097) (Fig. 5, light pink area). As for MIR elements, no difference was found between these regions and both regions only contained a few MIR elements (Fig. 5).

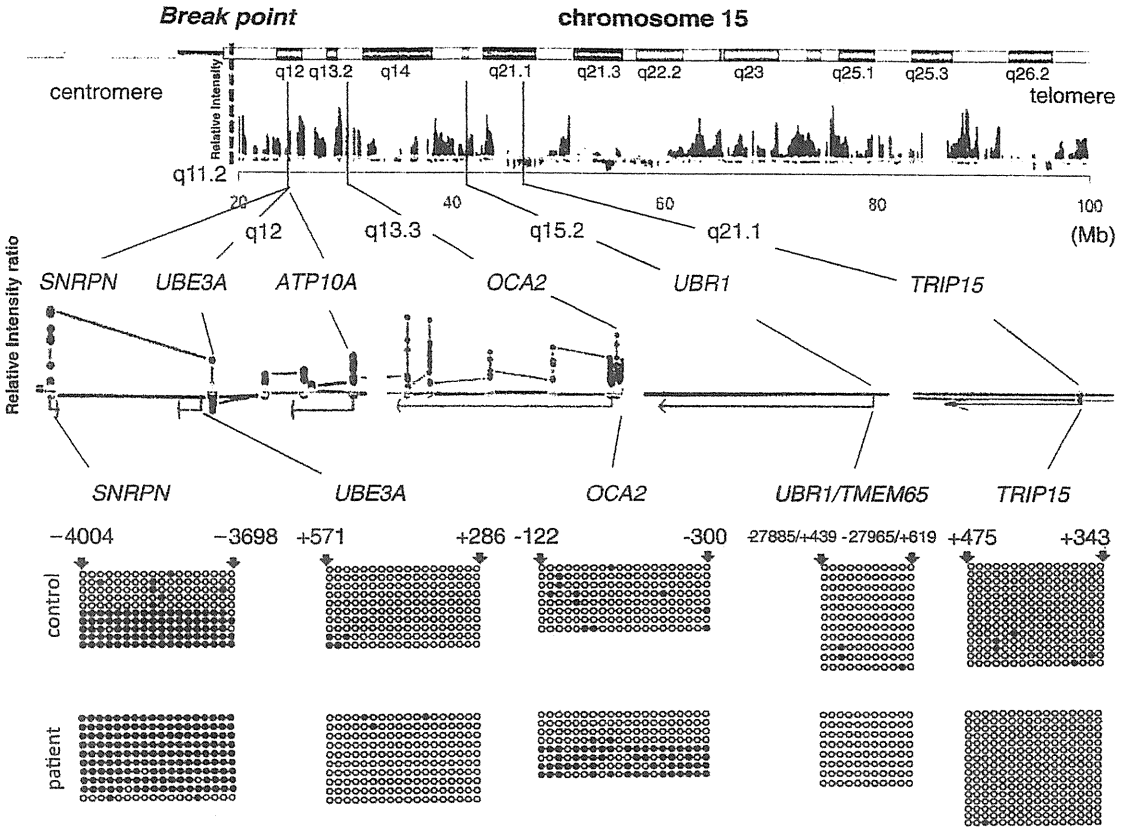

Fig. 4 DNA methylation analyses of CGIs in the chromosome 15 of the derivative X chromosome. *Upper panel*: profile of the DNA methylation difference between the chromosome 15 segment of the patient's derivative X chromosome and the chromosomes 15s of two healthy controls obtained by MeDIP analysis using CGI microarray analysis. *Middle panel*: enlarged view of the MeDIP analysis for genes on chromosome 15. *Spots* indicate the genomic positions of the oligonucleotides used for hybridization in the microarray assay, were designed within the CGIs of the genes. The *red arrows* indicate the transcriptional direction of the genes. The averages of hybridization determine the level of DNA methylation, which is shown as a *green* or *blue line*. *Lower panel*: bisulfite sequences of the CGIs on chromosome 15. *Open circle*: hypo-methylated CpG, *closed circle*: hypermethylated CpG. Genomic locations of the first and the last CpG in the sequence analyzed from the transcriptional start site are designated above the bisulfite sequence results

As expected, the CGIs of the genes in the distal region, *UBR1* and *TRIP15*, were not methylated (Fig. 4, middle and lower panels).

Distribution of transposable elements

We observed a high density of L1 elements in the upstream regions of the *SNRPN* and *OCA2* genes. However, the L1 density was low in the upstream region of the *UBE3A* gene. MIR elements were rarely detected in the upstream regions of all three genes. A high density of Alu transposable elements was observed in the upstream regions of the *SNRPN* gene, but not in the upstream regions of the *OCA2* and *UBE3A* genes.

Discussion

We molecularly characterized of the spread of XCI in an autosome of a boy with a t(X;15)(p21.1;q11.2) translocation. In this study, we found that (1) the *XIST* gene was active in the derivative X chromosome; (2) XCI and CGI hypermethylation constantly extended into the proximal region of the chromosome 15 section of the derivative X (breakpoint: ~15q14 [40 Mb from the centromere]); (3) CGI hypermethylation was not observed in the middle of 15q (15q21.1 [50 Mb]: q22.2 [60 Mb]); and (4) scattered CGI methylation was found in the distal 15q region (15q22.2 [60 Mb]: telomere). The CGI of *UBE3A* was not hypermethylated, although those of adjacent genes [e.g., the imprinted *SNRPN* gene and non-imprinted *ATP10A* (normally unmethylated)] (DuBose et al. 2010) were aberrantly hypermethylated. These results indicate that the spread of XCI from a translocated X chromosome is limited and gradually decreases (although it depends on the gene) in an autosome (Fig. 6).

As for the clinical relevance of these findings, the copy of Xq was completely inactivated in most of the cells, probably due to the selection of cells in which the derivative X

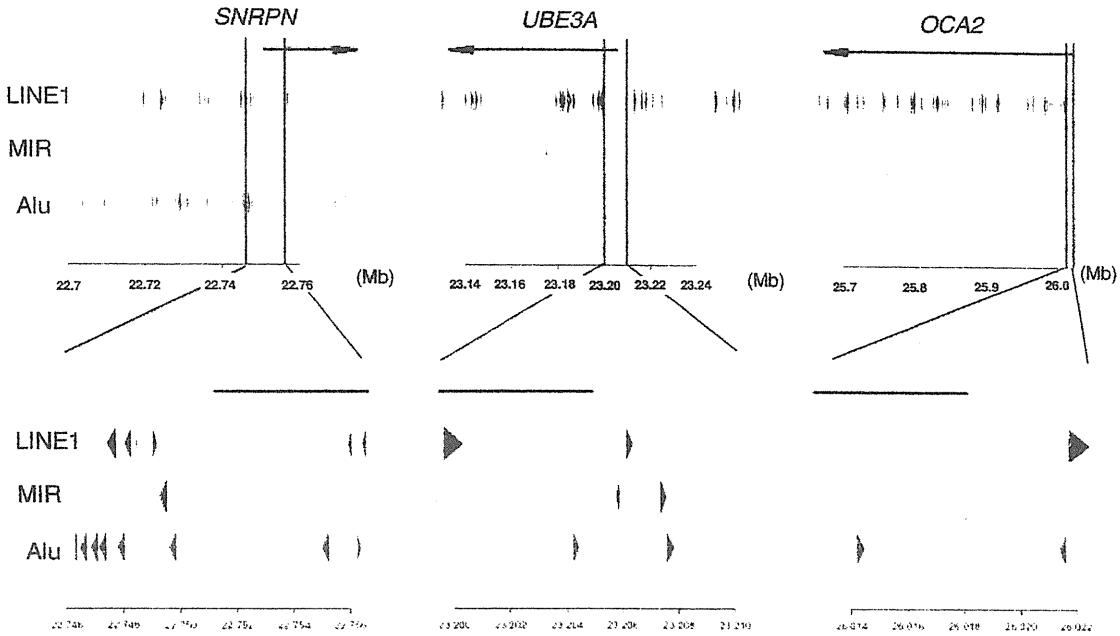

Fig. 5 Schematic illustration of the density of L1, MIR, and Alu repetitive sequences in the regions surrounding the transcription start sites of the *SNRPN*, *UBE3A*, and *OCA2* genes. A *triangle* (*red*, *black*, or *green*, respectively) indicates LINE1, MIR, or Alu sequences. The *direction* of each triangle indicates the transcriptional direction. The *SNRPN*, *UBE3A*, and *OCA2* gene regions are shown by the *arrows* at the *top*. The physical distance (Mb) from the telomere of the short arm of chromosome 15 is shown at the *bottom*

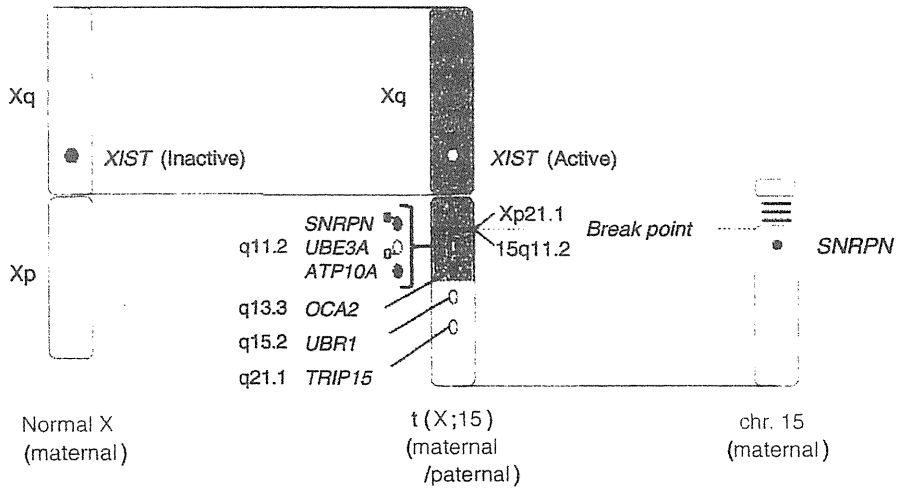

Fig. 6 Schematic representation of the molecular characterization of the patient with a t(X;15)(p21.1;q11.2) translocation. *Open circle* (*oval* and *hexagon*): hypo-methylated (active) gene, *closed circle* (*oval* and *hexagon*): hypermethylated (inactive) gene. *Open* and *closed squares* indicate low density and high density of LINE1 copies in the promoter regions of the genes, respectively

was active and the normal X was inactive during early development. Thus, some of the patient's clinical features should be due to gene inactivation caused by the spread of XCI, including *OCA2* and *SNRPN*, which may contribute to the hypo-pigmentation of the patient's skin and hair (Akahoshi et al. 2001; Brilliant et al. 1994) and the Prader–Willi syndrome-like features, respectively.

Wirth et al. reported a case with a translocation between chromosomes X and 15 [t(X;15)(q28;q12)]. In this case, the translocation was balanced (no monosomy), The XCI pattern was random (42:58), and XCI did not spread into the chromosome 15 part of the derivative X chromosome (Wirth et al. 2001). Because *SNRPN* and the adjacent *HBII-85* C/D box snoRNA (a transcript presumably related to the PWS phenotype) were disrupted by the breakpoint located in 15q12, the patient showed PWS-like features, such as obesity with an obsession for food, hypogonadism, and mental retardation at the age of 20 years, but did not have characteristic facial features, neonatal episodes of muscular hypotonia or failure to thrive. On the other hand, our patient's condition was more severe than the case of Wirth et al. and had features not described in that study, probably

because our patient not only had inactivation of the genes in the proximal chromosome 15 by XCI spread (including *SNRPN*) but also had a larger monosomic region of Xptel-p21.1, although the proportion of the cells, in which the der(X) was active, was small.

Several cases with XCI spread to the translocated autosome have been reported (Orellana et al. 2001; Sharp et al. 2001; Solari et al. 2001; Stankiewicz et al. 2006). Among these cases, the majority have shown the spread of XCI in an autosome (e.g., chromosomes 10, 14, and 15) (Orellana et al. 2001; Sharp et al. 2001; Stankiewicz et al. 2006). However, a few cases have not shown such a spread (e.g., chromosomes 2 and 21) (Solari et al. 2001). Thus, it may depend on the presence of certain features that facilitate XCI spread in the vicinity of the breakpoint on an autosome (Stankiewicz et al. 2006; Wirth et al. 2001). It has been suggested that XIST needs some sort of genomic "way station" to aid its spread, (Gartler and Riggs 1983) and that a certain class of transposons called long interspersed (LINE1 or L1) elements, (Lyon 1998) which are enriched on the X chromosome compared with autosomes, (Bailey et al. 2000; Popova et al. 2006) may be candidates for these way stations. It was recently discovered that LINE elements were expressed and their transcripts co-localize with the *XIst*-coated X chromosome during the X-inactivation time window in mice, LINE1 expression was observed in an autosome around an *Xist* gene that was integrated into a mouse autosome, and the efficiency of silencing by *Xist* correlates with the local concentration of full-length and truncated LINEs during the establishment and maintenance of inactivation (Chow et al. 2010). If these observations are true for each gene, then the "de novo" DNA methylation in the CGI of *SNRPN* and *OCA2* may represent the high silencing efficiency of *XIST* due to the high local concentration of LINE1, whereas the "escape from de novo DNA methylation" in the CGI of *UBE3A* may represent the low silencing efficiency of *XIST* due to the low local concentration of LINE1. Contrary to the situation with LINE1, Alu repetitive elements are thought to be more enriched in genes that escape inactivation (Wang et al. 2006) and, similar to LINE1, MIR elements are found at low levels in genes that escape inactivation (Ke and Collins 2003). However, our data did not support these hypotheses because *UBE3A* did not have a higher density of Alu repeats or a lower density of MIR elements than *SNRPN* in our study. Further extensive analysis at multiple distal genes will be necessary to elucidate the "way station" hypothesis in the spread of XCI in an autosome.

Since the HUMARA assay used in this study has an error rate <5% (Kubota et al. 1999), the patient's ratio (89:11) did not indicate a non-random (extremely skewed) XCI pattern. Thus, this result indicates the possible existence of a mosaic pattern and/or cells in which the derivative X is active. However, we did not find direct evidence for either of these possibilities, either by G-banding karyotyping (50 cells) or by replication R banding analysis (100 cells), respectively. If there are cells in which the derivative X is active and the normal X is inactive, then Xp (21.1-tel) monosomy can affect the phenotype; however, we did not observe the typical features described in females with Xp monosomy (Ogata et al. 1998), possibly because the proportion of these cells with an active derivative X and inactive normal X is low (~11%). It is also possible that some of the patient's features (e.g., cryptorchidism and hypogenitarism) may be caused by a Klinefelter-like karyotype, rather than inactivation of the PWS critical region on chromosome 15, since the patient had two X chromosomes and one Y chromosome (although one X chromosome is deleted between Xp21.1-p tel).

For the mechanism leading to the translocation, we can deduce that the initial event was a non-disjunction of the X chromosomes during maternal meiosis I, since the patient carried both maternal homologs. The translocation onto the X chromosome may be post-zygotic, given the juxtaposition of the paternal 15q on the maternal X chromosome. Furthermore, the absence of mosaicism, as determined from the cytogenetic (BrdU staining) and molecular (HUMARA assay) studies, imply the possibility that the translocation occurred very early during development, probably during the first post-zygotic divisions, as seen in a previous report (Orellana et al. 2001).

In summary, we demonstrated the extent and tendency of XCI spreading in an autosome in terms of DNA methylation using a microarray-based method. Further studies in different cases with t(X;A) translocations will contribute to a better understanding of the pathogenesis of congenital and acquired diseases, including hematological malignancies (Manola et al. 2007; Vassiliou et al. 2006) and may elucidate the properties of genes that determine whether they are subjected to or escape XCI.

Acknowledgments We thank the patient and their parents for their cooperation in this study and Professor Emeritus Tadashi Kajii for his critical reading of the manuscript. This research was supported in part by Grants-in-Aid for Scientific Research (S.S. and T.K.), Exploratory Research (T.K.) from the Ministry of Education, Culture Sports, Science, and Technology, Japan, and the Kawano foundation for medical research (T.K.), and Kawano Masanori Foundation for Promotion of Pediatrics (S.S.).

Conflict of interest None.

References

Akahoshi K, Fukai K, Kato A, Kimiya S, Kubota T, Spritz RA (2001) Duplication of 15q11.2-q14, including the P gene, in a woman with generalized skin hyperpigmentation. Am J Med Genet 104:299–302

Bailey JA, Carrel L, Chakravarti A, Eichler EE (2000) Molecular evidence for a relationship between LINE-1 elements and X chromosome inactivation: the Lyon repeat hypothesis. Proc Natl Acad Sci USA 97:6634–6639

Brilliant MH, King R, Francke U, Schuffenhauer S, Meitinger T, Gardner JM, Durham-Pierre D, Nakatsu Y (1994) The mouse pink-eyed dilution gene: association with hypopigmentation in Prader–Willi and Angelman syndromes and with human OCA2. Pigment Cell Res 7:398–402

Brown CJ, Ballabio A, Rupert JL, Lafreniere RG, Grompe M, Tonlorenzi R, Willard HF (1991) A gene from the region of the human X inactivation centre is expressed exclusively from the inactive X chromosome. Nature 349:38–44

Chow JC, Ciaudo C, Fazzari MJ, Mise N, Servant N, Glass JL, Attreed M, Avner P, Wutz A, Barillot E, Greally JM, Voinnet O, Heard E (2010) LINE-1 activity in facultative heterochromatin formation during X chromosome inactivation. Cell 141:956–969

DuBose AJ, Johnstone KA, Smith EY, Hallett RA, Resnick JL (2010) Atp10a, a gene adjacent to the PWS/AS gene cluster, is not imprinted in mouse and is insensitive to the PWS-IC. Neurogenetics 11:145–151

Gartler SM, Riggs AD (1983) Mammalian X-chromosome inactivation. Annu Rev Genet 17:155–190

Giorda R, Bonaglia MC, Milani G, Baroncini A, Spada F, Beri S, Menozzi G, Rusconi M, Zuffardi O (2008) Molecular and cytogenetic analysis of the spreading of X inactivation in a girl with microcephaly, mild dysmorphic features and t(X;5)(q22.1;q31.1). Eur J Hum Genet 16:897–905

Herzing LB, Romer JT, Horn JM, Ashworth A (1997) Xist has properties of the X-chromosome inactivation centre. Nature 386:272–275

Ke X, Collins A (2003) CpG islands in human X-inactivation. Ann Hum Genet 67:242–249

Kubota T, Nonoyama S, Tonoki H, Masuno M, Imaizumi K, Kojima M, Wakui K, Shimadzu M, Fukushima Y (1999) A new assay for the analysis of X-chromosome inactivation based on methylation-specific PCR. Hum Genet 104:49–55

Kubota T, Wakui K, Nakamura T, Ohashi H, Watanabe Y, Yoshino M, Kida T, Okamoto N, Matsumura M, Muroya K, Ogata T, Goto Y, Fukushima Y (2002) The proportion of cells with functional X disomy is associated with the severity of mental retardation in mosaic ring X Turner syndrome females. Cytogenet Genome Res 99:276–284

Lee JT, Jaenisch R (1997) Long-range cis effects of ectopic X-inactivation centres on a mouse autosome. Nature 386:275–279

Lee JT, Strauss WM, Dausman JA, Jaenisch R (1996) A 450 kb transgene displays properties of the mammalian X-inactivation center. Cell 86:83–94

Lyon MF (1961) Gene action in the X-chromosome of the mouse (*Mus musculus* L.). Nature 190:372–373

Lyon MF (1962) Sex chromatin and gene action in the mammalian X-chromosome. Am J Hum Genet 14:135–148

Lyon MF (1998) X-chromosome inactivation: a repeat hypothesis. Cytogenet Cell Genet 80:133–137

Manola KN, Stavropoulou C, Georgakakos VN, Zoi K, Fisfis M, Evmorfiadis I, Zoi C, Pantelias GE, Stefanoudaki K, Sambani C (2007) Switch in X-inactivation in a JAK2 V617F-negative case of polycythemia vera with two acquired X-autosome translocations. Leuk Res 31:1009–1014

Ogata T, Wakui K, Muroya K, Ohashi H, Matsuo N, Brown DM, Ishii T, Fukushima Y (1998) Microphthalmia with linear skin defects syndrome in a mosaic female infant with monosomy for the Xp22 region: molecular analysis of the Xp22 breakpoint and the X-inactivation pattern. Hum Genet 103:51–56

Orellana C, Martinez F, Badia L, Millan JM, Montero MR, Andres J, Prieto F (2001) Trisomy rescue by postzygotic unbalanced (X;14) translocation in a girl with dysmorphic features. Clin Genet 60:206–211

Popova BC, Tada T, Takagi N, Brockdorff N, Nesterova TB (2006) Attenuated spread of X-inactivation in an X;autosome translocation. Proc Natl Acad Sci USA 103:7706–7711

Schmidt M, Du Sart D (1992) Functional disomies of the X chromosome influence the cell selection and hence the X inactivation pattern in females with balanced X-autosome translocations: a review of 122 cases. Am J Med Genet 42:161–169

Sharp A, Robinson DO, Jacobs P (2001) Absence of correlation between late-replication and spreading of X inactivation in an X;autosome translocation. Hum Genet 109:295–302

Sharp AJ, Spotswood HT, Robinson DO, Turner BM, Jacobs PA (2002) Molecular and cytogenetic analysis of the spreading of X inactivation in X;autosome translocations. Hum Mol Genet 11:3145–3156

Sharp AJ, Migliavacca E, Dupre Y, Stathaki E, Sailani MR, Baumer A, Schinzel A, Mackay DJ, Robinson DO, Cobellis G, Cobellis L, Brunner HG, Steiner B, Antonarakis SE (2010) Methylation profiling in individuals with uniparental disomy identifies novel differentially methylated regions on chromosome 15. Genome Res 20:1271–1278

Solari AJ, Rahn IM, Ferreyra ME, Carballo MA (2001) The behavior of sex chromosomes in two human X-autosome translocations: failure of extensive X-inactivation spreading. Biocell 25:155–166

Stankiewicz P, Kuechler A, Eller CD, Sahoo T, Baldermann C, Lieser U, Hesse M, Glaser C, Hagemann M, Yatsenko SA, Liehr T, Horsthemke B, Claussen U, Marahrens Y, Lupski JR, Hansmann I (2006) Minimal phenotype in a girl with trisomy 15q due to t(X;15)(q22.3;q11.2) translocation. Am J Med Genet A 140:442–452

Takagi N, Abe K (1990) Detrimental effects of two active X chromosomes on early mouse development. Development 109:189–201

Uehara S, Hanew K, Harada N, Yamamori S, Nata M, Niikawa N, Okamura K (2001) Isochromosome consisting of terminal short arm and proximal long arm X in a girl with short stature. Am J Med Genet 99:196–199

Vassiliou GS, Campbell PJ, Li J, Roberts I, Swanton S, Huntly BJ, Fourouclas N, Baxter EJ, Munro LR, Culligan DA, Scott LM, Green AR (2006) An acquired translocation in JAK2 Val617Phe-negative essential thrombocythemia associated with autosomal spread of X-inactivation. Haematologica 91:1100–1104

Wang Z, Willard HF, Mukherjee S, Furey TS (2006) Evidence of influence of genomic DNA sequence on human X chromosome inactivation. PLoS Comput Biol 2:e113

White WM, Willard HF, Van Dyke DL, Wolff DJ (1998) The spreading of X inactivation into autosomal material of an x;autosome translocation: evidence for a difference between autosomal and X-chromosomal DNA. Am J Hum Genet 63:20–28

Wirth J, Back E, Huttenhofer A, Nothwang HG, Lich C, Gross S, Menzel C, Schinzel A, Kioschis P, Tommerup N, Ropers HH, Horsthemke B, Buiting K (2001) A translocation breakpoint cluster disrupts the newly defined 3′ end of the SNURF-SNRPN transcription unit on chromosome 15. Hum Mol Genet 10:201–210

Xue F, Tian XC, Du F, Kubota C, Taneja M, Dinnyes A, Dai Y, Levine H, Pereira LV, Yang X (2002) Aberrant patterns of X chromosome inactivation in bovine clones. Nat Genet 31:216–220

Yang X, Smith SL, Tian XC, Lewin HA, Renard JP, Wakayama T (2007) Nuclear reprogramming of cloned embryos and its implications for therapeutic cloning. Nat Genet 39:295–302